

Early Mitochondrial Dysfunction in Long-lived *Mclk1*^{+/-} Mice*

Received for publication, April 30, 2008, and in revised form, July 17, 2008 Published, JBC Papers in Press, July 17, 2008, DOI 10.1074/jbc.M803287200

Jérôme Lapointe and Siegfried Hekimi¹

From the Department of Biology, McGill University, Montreal H3A 1B1, Canada

Reduced activity of CLK-1/MCLK1 (also known as COQ7), a mitochondrial enzyme that is necessary for ubiquinone biosynthesis, prolongs the lifespan of nematodes and mice by a mechanism that is distinct from that of the insulin signaling pathway. Here we show that 2-fold reduction of MCLK1 expression in mice reveals an additional function for the protein, as this level of reduction does not affect ubiquinone levels yet affects mitochondrial function substantially. Indeed, we observe that the phenotype of young *Mclk1*^{+/-} mutants includes a severe reduction of mitochondrial electron transport, ATP synthesis, and total nicotinamide adenine dinucleotide (NAD_{tot}) pool size as well as an alteration in the activity of key enzymes of the tricarboxylic acid cycle. Surprisingly, we also find that *Mclk1* heterozygosity leads to a dramatic increase in mitochondrial oxidative stress by a variety of measures. Furthermore, we find that the mitochondrial dysfunction is accompanied by a decrease in oxidative damage to cytosolic proteins as well as by a decrease in plasma isoprostanes, a systemic biomarker of oxidative stress and aging. We propose a mechanism for the conjunction of low ATP levels, high mitochondrial oxidative stress, and low non-mitochondrial oxidative damage in a long-lived mutant. Our model helps to clarify the relationship between energy metabolism and the aging process and suggests the need for a reformulation of the mitochondrial oxidative stress theory of aging.

Mutational inactivation of *clk-1* in *Caenorhabditis elegans* (1) and partial inactivation of its orthologue *Mclk1* in mice (2) prolong average and maximum lifespan in these organisms. Genetic evidence in nematodes indicates that the mechanism by which *clk-1* prolongs lifespan is distinct from that of the insulin signaling pathway but overlaps with that of caloric restriction (3, 4), which makes the *clk-1/Mclk1*-dependent mechanism one of the very few molecularly defined and evolutionarily conserved pathways of animal aging that has been found to affect mammals (5–7). CLK-1/MCLK1 is a mitochondrial hydroxylase that is necessary for the biosynthesis of ubiquinone (coenzyme Q or UQ), a membrane antioxidant, lipid soluble enzymatic cofactor, and essential electron trans-

porter of the mitochondrial respiratory chain (8, 9). In the absence of CLK-1/MCLK1, both worms and cultured mouse ES cells accumulate the biosynthetic intermediate demethoxyubiquinone (DMQ).² Furthermore, no UQ can be detected in *Mclk1*^{-/-} embryos, which start to die after embryonic day 8 (8). In contrast, *clk-1* mutant worms, although they are equally unable to manufacture UQ₉, survive thanks to their ability to absorb dietary (bacterial) UQ₈ (endogenous UQ₉ and bacterial UQ₈ have different isoprenoid side chain lengths, as indicated by the subscript). These mutants, therefore, contain a mix of exogenous UQ₈ and endogenous DMQ₉. In such animals, Kayser *et al.* (10) discovered a reduction in electron transport from mitochondrial complex I but not from complex II, an observation that was interpreted as a difference in the way these complexes interact with the quinone pool. In contrast, in *Mclk1*^{-/-} mouse ES cells, which contain DMQ₉ but no detectable level of exogenous UQ, only electron transport from complex II is impaired (8).

Molecular and genetic analysis of different alleles of *C. elegans clk-1* has previously suggested that CLK-1 might have other roles in mitochondrial function in addition to that of a DMQ hydroxylase. In particular, it was found that both the phenotypically severe allele *clk-1(qm30)*, a partial deletion that does not produce any CLK-1 protein, and the phenotypically weaker allele *clk-1(e2519)*, a Glu to Lys missense mutation that produces wild-type levels of a full-length mutant protein (11), are equally unable to sustain UQ biosynthesis (12). Furthermore, suppression of *clk-1(e2519)* by a tRNA missense suppressor produces only very small amounts of UQ₉, but results in full phenotypic suppression (13). Together these observations suggest that at least part of the phenotype of *clk-1* mutants is not because of the defect in UQ biosynthesis.

Previous analysis of *Mclk1*^{+/-} mutants revealed that the level of MCLK1 protein was reduced ~2-fold in these animals and that their lifespan was increased up to 30% compared with that of their *Mclk1*^{+/+} siblings in three distinct genetic backgrounds (2). It was also discovered that in the livers of very old *Mclk1*^{+/-} mutants, analyzed shortly before natural death, there are areas of complete loss of expression of *Mclk1*, both mRNA and protein, through a phenomenon of loss-of-heterozygosity (2). We and others (14) have speculated that the presence of these *Mclk1*^{-/-} clones might be responsible for the longevity of *Mclk1*^{+/-} mutants. However, because *Mclk1*^{-/-} clones have been found exclusively in very old animals, the notion of their

* This study was funded in part by a grant from the National Science and Engineering Research Council of Canada. The costs of publication of this article were defrayed in part by the payment of page charges. This article must therefore be hereby marked "advertisement" in accordance with 18 U.S.C. Section 1734 solely to indicate this fact.

¹ Holds the Robert Archibald and Catherine Louise Campbell Chair of Developmental Biology. To whom correspondence should be addressed: Dept. of Biology, McGill University, 1205 Ave. Docteur Penfield, Montreal H3A 1B1, Canada. Tel.: 514-398-6440; E-mail: Siegfried.Hekimi@McGill.ca.

² The abbreviations used are: DMQ, demethoxyubiquinone; TCA, tricarboxylic acid; HPLC, high performance liquid chromatography; TMPD, *N,N,N',N'*-tetramethyl-*p*-phenylenediamine; ROS, reactive oxygen species.

Defective Mitochondria in Long-lived Mice

importance for the extended lifespan of these animals implies that the extension is the result of a protective effect that takes place in old animals only and not the result of a reduction of the rate of aging throughout life.

In the present study we have tested various aspects of the phenotype of young *Mclk1*^{+/-} mutants, with particular attention to mitochondria, to better understand the basis of the increased longevity of these animals. We demonstrate that the reduction of MCLK1 levels in young *Mclk1*^{+/-} animals does not affect UQ levels yet profoundly alters the functions of the electron transport chain and the tricarboxylic acid (TCA) cycle while increasing mitochondrial oxidative stress. Additionally, we show that this early mitochondrial dysfunction leads to a reduction in the levels of cytosolic oxidative damage to proteins (protein carbonyls) as well as in a reduction in the levels of a systemic biomarker of aging (plasma isoprostanes), thus suggesting that the anti-aging effect triggered by low MCLK1 levels already occurs at a young age. These results provide a genetic model that will help to clarify the links between mitochondrial function and aging.

EXPERIMENTAL PROCEDURES

Animals—All the animals were housed in a pathogen-free facility at McGill University and were given a standard rodent diet and water *ad libitum*. Mice, 3-month-old Balb/c males, were anesthetized, sacrificed by cervical dislocation, and perfused with phosphate buffer. Tissues were then rapidly removed, rinsed, and placed in ice-cold mitochondrial isolation buffer or immediately frozen in liquid nitrogen. All procedures were approved by the McGill Animal Care and Ethics committees.

Identification of Quinones—The extraction of quinones as well as their quantification by HPLC were performed as we previously described (2). The total amount of quinone was normalized to the amount of protein.

Mitochondrial Oxygen Consumption and ATP Production—Unless otherwise stated, all the chemicals and reagents were purchased from Sigma. On the day of the experiment, fresh tissues were homogenized in 10 volumes (w/v) of the indicated homogenization buffer: 0.25 M sucrose, 10 mM Hepes buffer, pH 7.4, 1 mM EDTA (for liver and kidney); 100 mM sucrose, 10 mM EDTA, 100 mM Tris-HCl, pH 7.4, 46 mM KCl, 0.5% bovine serum albumin (BSA) (for muscle); 220 mM mannitol, 70 mM sucrose, 10 mM Hepes, pH 7.4, 1 mM EGTA, 0.04 mM BSA (for heart); 75 mM sucrose, 5 mM Hepes, pH 7.4, 1 mM EGTA (for brain). Mitochondria were isolated by standard differential centrifugation according to detailed procedures described elsewhere (15–18). The purity of the mitochondrial and cytosolic preparations obtained by following the published methods were checked by classic Western blotting experiments with antisera against mitochondrial porin (Calbiochem) and cytosolic α -tubulin. No porin and no α -tubulin could be detected in the cytosolic and the mitochondrial fractions respectively (Fig. 2A). Oxygen consumption of isolated mitochondria was measured polarographically with a Clark-type oxygen electrode connected to a suitable recorder (Yellow Springs instruments) in a 1.75-ml thermostatted water-jacketed closed chamber with magnetic stirring at 30 °C according to Schuh *et al.* (19) with

some modifications. Briefly, the respiratory reaction medium consisted of 250 mM sucrose, 10 mM HEPES, pH 7.2, 20 mM KCl, 5 mM KH₂PO₄, and 2 mM MgCl₂. Mitochondria were added to a final concentration of 0.5 mg protein/ml with external electron donor substrates consisting of either 5 mM glutamate or pyruvate (with 1 mM malate), 5 mM succinate (with 1 μ M rotenone), or 0.15 mM *N,N,N',N'*-tetramethyl-*p*-phenylenediamine (TMPD, with 2.5 mM ascorbate and 1 μ M antimycin). Mitochondrial oxygen consumption in the presence of substrates and ADP (0.8 mM) is reported as state 3, whereas the state corresponding to the period after all added ADP has been converted into ATP is defined as State 4 respiration. State 4 respiration was also measured in the presence of 1.25 mg/ml oligomycin to eliminate the contribution of ATP cycling enzymes. The respiratory control ratio (state 3/state 4) of control animals was \sim 7.5 with glutamate/malate and \sim 4 with succinate plus rotenone, indicating intactness of the inner mitochondrial membrane. We also evaluated the coupling between ADP phosphorylation and oxygen consumption by calculating the adenosine diphosphate-to-oxygen ratio (ADP/O) from the trace graph (Fig. 2B), and the resulting data, \sim 3.2 for glutamate/malate and \sim 2 for succinate + rotenone, indicated that the control mitochondria were well coupled. The fully uncoupled rate of oxygen consumption was also measured after the addition of 1 μ M carbonyl cyanide *p*-trifluoromethoxyphenylhydrazone, and no difference was observed between control and heterozygous animals (not shown). The quality of mitochondria preparation was confirmed by at least a 3-fold increase in respiration rate in the presence of the uncoupler. The quantification of ATP synthesis by isolated mitochondria was performed according to the method previously described by Drew and Leeuwenburgh (20) and using the ATP determination kit (Invitrogen) for quantitatively measuring ATP production. After the initial luminescence reading, ADP (200 μ M) was added to the respiratory reaction medium containing freshly isolated mitochondria (0.5 mg/ml), and the increase in luminescence was monitored for 2 min at 30-s intervals on an infinite M200 plate reader (Tecan).

Quantitative Determination of Mitochondrial and Tissue ATP, ADP, and Total NAD Levels—Mitochondrial and tissue adenine nucleotides (ADP and ATP) levels were determined using an ATP determination kit (Invitrogen) as described elsewhere (21). Total nicotinamide adenine dinucleotide (NAD, NADH) levels were determined using the NAD⁺/NADH quantification kit (Biovision) according to the manufacturer's instructions. Standard curves generated with known amounts of purified ATP and NADH were used to calculate mitochondrial and tissue concentrations.

Electron Transport Chain Assays—Mitochondrial samples were diluted with 30 mM potassium phosphate, pH 7.4, to reach a concentration of about 1 mg/ml protein concentration and then subjected to three rounds of freezing-thawing. Activities of the respiratory chain enzymes and levels of electron transport were measured at 30 °C using a Beckman DU 640 spectrophotometer as described (22). All reactions were initiated by the addition of mitochondrial proteins, complex I (10 μ g), complex II (15 μ g), complex III (10 μ g), complex IV (5 μ g), complex I-II (5 μ g), and complex II-III (5 μ g). For complex II activity,

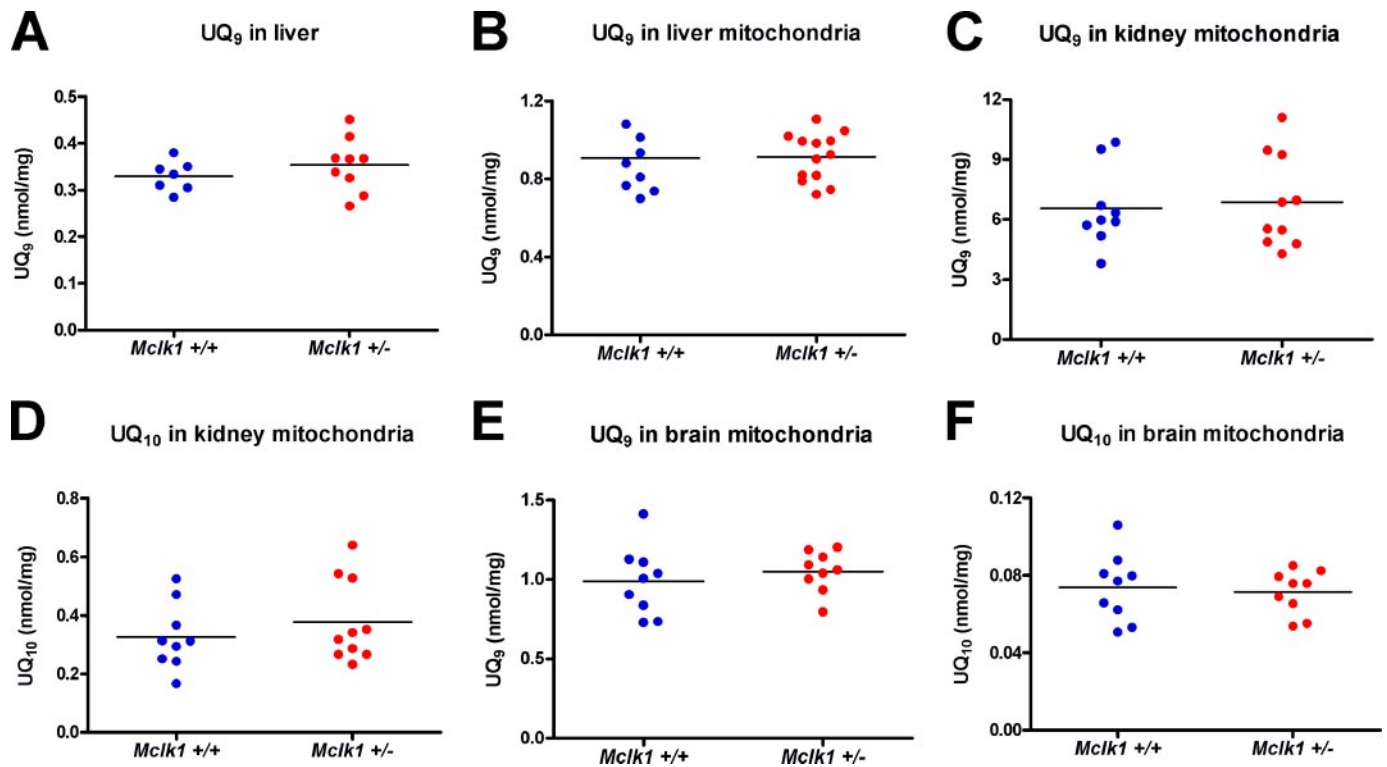


FIGURE 1. Ubiquinone levels are normal in *Mcl1k1*^{+/-} mice. A, quantification of UQ₉ levels in whole liver homogenates from 3-month-old *Mcl1k1*^{+/+} and *Mcl1k1*^{+/-} Balb/c males was performed by HPLC analysis. B, UQ₉ levels in isolated liver mitochondria from 3-month-old *Mcl1k1*^{+/+} and *Mcl1k1*^{+/-} males. UQ₁₀ is barely detectable in liver (not shown). C–F, UQ₉ and UQ₁₀ levels in kidney and brain mitochondria from 3-month-old *Mcl1k1*^{+/+} and *Mcl1k1*^{+/-} Balb/c males. Each dot in the graphs represents an individual mouse.

activity was measured by following the decrease in absorbance due to the coupled reduction of 2,6-dichlorophenolindophenol at 600 with 750 nm as the reference wavelength. The reaction mixture containing 50 mM potassium phosphate, pH 7.4, 20 mM succinate, and 5 mM MgCl₂ was preincubated with 15 μg of mitochondrial protein at 30 °C. After 10 min of incubation, antimycin (2 μg), rotenone (2 μg), KCN (2 mM), and 2,6-dichlorophenolindophenol (150 μM) were added. 2,6-Dichlorophenolindophenol can accept electrons from the complex II (23), the complex II-bound ubiquinone, or exogenous ubiquinone. Thus, the activity was first monitored for 1 min without the addition of exogenous ubiquinone. Subsequently, complex II activity was also measured with the addition of ubiquinone (Q₁) (100 μM) and was monitored for 2 min. No difference was observed between both genotypes with the addition of exogenous Q₁ to the reaction.

Assay of TCA Cycle Enzymes—Activities of TCA cycle enzymes (citrate synthase, aconitase, isocitrate dehydrogenase, α-ketoglutarate dehydrogenase, and malate dehydrogenase) in mitochondrial preparations were measured as previously described (24).

H₂O₂ Production—Hydrogen peroxide (H₂O₂) production from isolated liver mitochondria was measured fluorimetrically utilizing the Amplex RedTM-horseradish peroxidase method (Invitrogen) as previously described (25) with some modifications. Briefly, the reaction medium contained 125 mM KCl, 2 mM MgCl₂, 0.2 mM EGTA, 2 mM KH₂PO₄, 10 mM HEPES, pH 7.2, 5 units/ml horseradish peroxidase, 20 units/ml superoxide dismutase, and 1 μM Amplex Red. After mitochondrial addi-

tion, the oxidizable substrate consisting of 5 mM glutamate plus malate was added. Adenosine diphosphate (0.8 mM) was added a minute later followed by oligomycin (1.25 μg/ml). Detection of H₂O₂ production was measured as an increase in fluorescence of Amplex Red dye at 590 nm with the excitation wavelength set at 545 nm. The dye response was calibrated with the addition of known amounts of H₂O₂.

Enzymatic Antioxidant Assays—Mitochondrial and cytosolic Se-GPx activities were determined by the standard indirect method of NADPH oxidation using *t*-butyl hydroperoxide (26). Manganese-dependent and CuZn-superoxide dismutase activities were assessed using a commercially available kit (Cayman Chemical).

ROS Damage—Lipid peroxidation was determined by the indirect measurement of free aldehydes, malondialdehydes plus 4-hydroxyalkenals such as 4-hydroxy-2(*E*)nonenal, using a commercially available kit (LPO-586, OxisResearch). The level of protein carbonyl in liver tissues was determined with the Protein Carbonyl Assay kit (Cayman Chemical) according to manufacturer's instructions. Plasma free and esterified 8-isoprostanes were quantified with an 8-isoprostanes enzyme immunoassay kit (Cayman Chemical) according to the provided protocol. The plasma levels of 8-hydroxy-2-deoxyguanosine, a biomarker for oxidative damage to DNA, were determined using an enzyme-linked immunosorbent assay kit according to the manufacturer's protocol (Stressgen).

Statistical Analysis—Analyses were performed using an unpaired two-tailed Student's *t* test, and differences between the two genotypes (10–12 *Mcl1k1*^{+/+} and *Mcl1k1*^{+/-} animals

Defective Mitochondria in Long-lived Mice

unless otherwise stated in the figure legends) were considered to be significant when p was <0.05 .

RESULTS

Reduction in Mitochondrial Electron Transport between Mitochondrial Complexes Despite Normal Levels of Ubiquinone—We have shown previously that *Mclk1*^{+/-} tissues exhibit the expected 2-fold decrease in *Mclk1* mRNA and MCLK1 protein levels but that UQ₉ levels were unaffected in tissue homogenates from such mice (2, 8). We have now extended these studies to mitochondrial extracts, which we also find to display no reduction in either UQ₉ or UQ₁₀ levels in either of the liver, kidney, or brain of the very animals used in the various studies described below (Fig. 1). This suggests that *Mclk1* is in fact fully recessive for its function in UQ biosynthesis. However, as we have found that the heterozygous mice have an extended lifespan, and for other reasons outlined in the introduction, there are grounds to believe that CLK-1/MCLK1 could also have an additional activity unrelated to UQ biosynthesis (13) but responsible for the phenotypes observed in *Mclk1*^{+/-} heterozygous mutants.

As MCLK1 is a mitochondrial protein, we tested various aspects of mitochondrial function in young (3 months old) Balb/c *Mclk1*^{+/-} males in five representative organs. We found that in liver (Fig. 2, B and C) and kidney (Fig. 2D), the rate of electron transport measured by oxygen consumption from intact isolated mitochondria is reduced with both complex I substrates (glutamate in combination with malate) and a complex II substrate (succinate) as well as with an artificial substrate (TMPD plus ascorbate) that donates electrons directly to cytochrome *c* and, thus, measures electron transport from cytochrome *c* to complex IV (27). Similar results were observed with *Mclk1*^{+/-} males from the C57BL/6J and the 129SV/j X Balb/c genetic backgrounds (data not shown). We also tested electron transport between pairs of com-

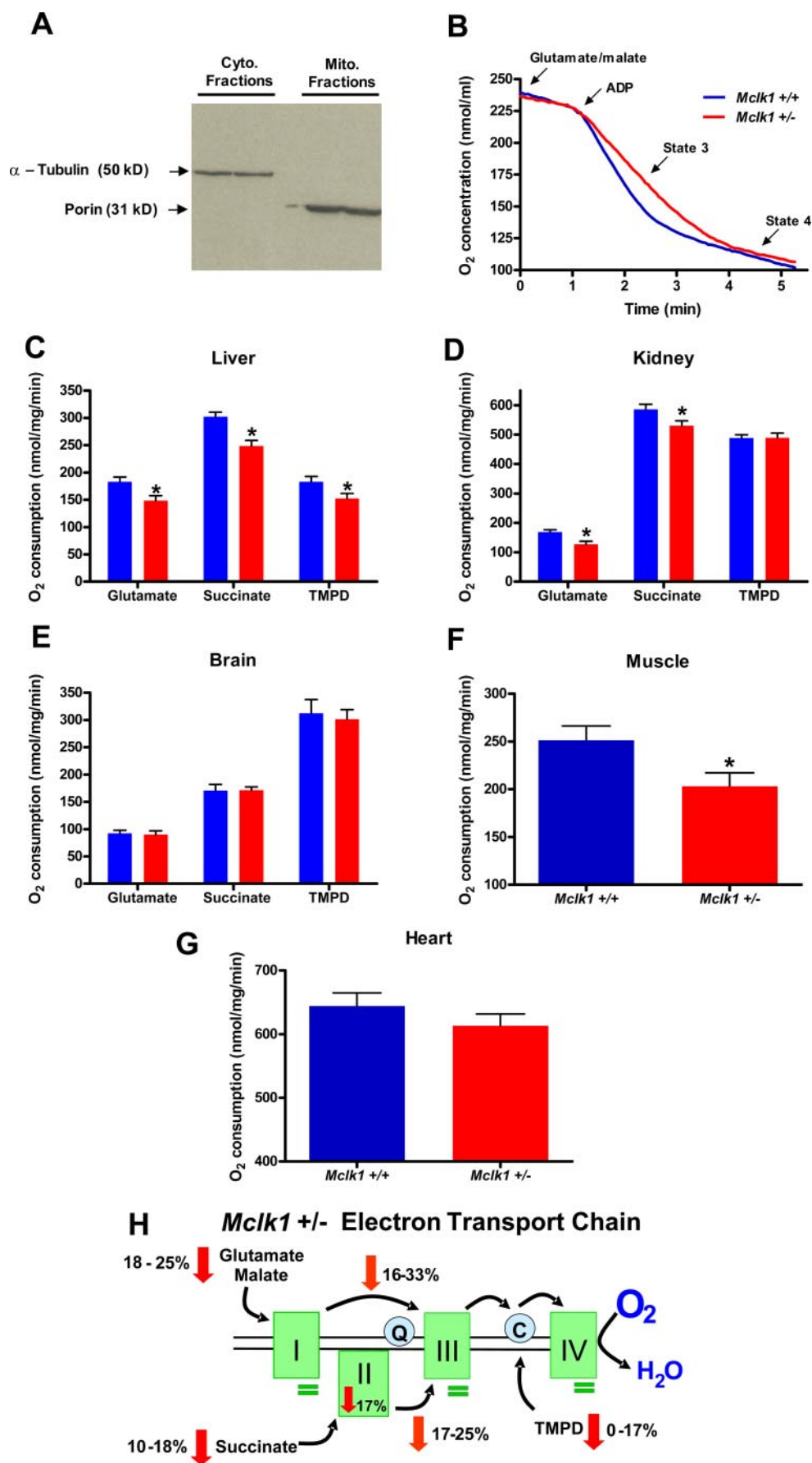


TABLE 1
Mitochondrial electron transport chain and TCA cycle-related measurements

ND, not determined.

	Liver		Kidney		Brain	
	<i>Mclk1</i> ^{+/+}	<i>Mclk1</i> ^{+/-}	<i>Mclk1</i> ^{+/+}	<i>Mclk1</i> ^{+/-}	<i>Mclk1</i> ^{+/+}	<i>Mclk1</i> ^{+/-}
	nmol/mg/min		nmol/mg/min		nmol/mg/min	
Electron transport chain assays						
C I ^a	144 ± 14 ^b	136 ± 8	211 ± 7	218 ± 7	182 ± 8	200 ± 9
C II	53 ± 4	41 ± 4 ^c	215 ± 5	192 ± 6 ^c	118 ± 10	113 ± 13
C III	261 ± 35	254 ± 19	262 ± 16	265 ± 15	748 ± 30	765 ± 30
C IV	207 ± 10	220 ± 16	213 ± 14	233 ± 17	736 ± 29	754 ± 21
C I-III	263 ± 33	178 ± 16 ^c	1007 ± 34	852 ± 23 ^c	467 ± 27	483 ± 26
C II-III	267 ± 28	201 ± 9 ^c	427 ± 17	355 ± 13 ^c	210 ± 13	234 ± 7
TCA cycle enzymes						
Citrate S.	106 ± 8	95 ± 8	ND	ND	ND	ND
Aconitase	21.3 ± 1	16 ± 1.1 ^c	ND	ND	ND	ND
α-KGDH	10.9 ± 1.2	15.9 ± 1.4 ^c	56.2 ± 3.7	71.6 ± 3.7 ^c	39.7 ± 2	41.2 ± 4
Iso. D.	29.1 ± 5.3	33.1 ± 2.8	ND	ND	ND	ND
Malate D.	3570 ± 281	3261 ± 210	ND	ND	ND	ND
GDH	354 ± 77	290 ± 37	875 ± 31	892 ± 33	509 ± 42	561 ± 34

^a C I-IV, mitochondrial complexes; C I-III and C II-III, electron transport between complexes; Citrate S., citrate synthase; α-KGDH, α-ketoglutarate dehydrogenase; Iso. D., isocitrate dehydrogenase; Malate D., malate dehydrogenase; GDH, glutamate dehydrogenase.

^b Data are the means ± S.E. of 10–15 samples.

^c Statistically significant at $p < 0.05$.

plexes (complex I to III and complex II to III) and found decreases in electron transport of a similar magnitude as for overall electron transport measured by oxygen consumption (Table 1; Fig. 2H). In addition, we tested oxygen consumption with glutamate in skeletal muscle and heart (Fig. 2, F and G). A clear decrease of oxygen consumption was observed in skeletal muscle similar to that seen in liver and kidney, and a similar trend was also observed in heart mitochondria. The reduction in electron transport in *Mclk1*^{+/-} mutants in the absence of any reduction in UQ levels in these animals indicates that partial loss of MCLK1 affects electron transport independently of the function of the protein in UQ biosynthesis. This conclusion is also consistent with the finding of a reduction of electron transport from cytochrome *c* to complex IV, a step that does not require UQ.

Using specific electron donors and acceptors we also tested the activities of complexes I through IV individually (Table 1 and Fig. 2H). In liver and kidney the activity of all complexes appeared essentially intact in the *Mclk1*^{+/-} mutants. Only complex II is affected in *Mclk1*^{+/-} mice but only when no soluble UQ₁ is provided as a mediator to enhance electron transport to the oxidized acceptor (see “Experimental Procedures”). This suggests that there is a very mild defect in the mutant complex that can only be revealed under conditions in which electron transport by the complex cannot be efficient.

Interestingly, the defects in mitochondrial function that we describe were not observed in the brain (Fig. 2E). Brain mitochondrial function is known to be quite different from that of

non-nervous tissue as is also apparent from our measurements of the wild type (Table 1). Further experiments will be necessary to determine why brain mitochondria are immune to a partial loss of MCLK1 function.

Reduction in the Rate of Mitochondrial ATP Synthesis, in Cellular ATP, and in Total Nicotinamide Adenine Dinucleotide Levels—The main function of mitochondrial electron transport is ATP production. We, therefore, determined the rate of ATP synthesis from liver mitochondria (Fig. 3A). We observed a marked decrease in the rate of ATP synthesis that correlated strongly with the rate of oxygen consumption in preparations from individual animals (Fig. 3B). We also measured ATP levels in the freshly isolated mitochondria at the beginning of the experiment (Fig. 3C) and observed a reduction in these levels. This suggests that ATP synthesis is reduced *in vivo*; that is, even when the mitochondria are not provided with saturating amounts of substrate, ADP, and oxygen, as is the case *in vitro*. We confirmed this observation by measuring ATP levels in samples of snap-frozen livers, kidneys, and hearts and observed strikingly lower ATP levels in all three organs (Fig. 3D). This decrease in ATP levels results in a lower ATP/ADP ratio in liver (Fig. 3E). Of note, the difference in absolute ATP levels between tissues and isolated mitochondria is likely attributable to a loss of ATP content that is known to occur during the isolation procedure (28). One crucial ATP-dependent cellular process that impinges on energy metabolism and many other processes is the biosynthesis of nicotinamide adenine dinucleotides (including NAD⁺ and NADH). We, therefore, determined the total NAD level in frozen liver and found it to be significantly lower

FIGURE 2. Reduction of MCLK1 levels alters mitochondrial function in young *Mclk1*^{+/-} mice. A, purity of cytosolic and mitochondrial fractions was assessed by Western blotting with antisera against cytosolic (Cyto.) α-tubulin and mitochondrial (Mito.) porin. B, typical trace graph representing oxygen consumption by *Mclk1*^{+/+} and *Mclk1*^{+/-} liver mitochondria after glutamate/malate addition in respiratory reaction medium. Oxygen consumption levels of isolated liver (C), kidney (D), and brain (E) mitochondria from young (3 months) males were measured with glutamate/malate, succinate, and TMPD as specific respiratory substrates. Results with *Mclk1*^{+/+} are represented with blue bars, and those with *Mclk1*^{+/-} are represented with red bars. For muscle (F) and heart (G) mitochondria, respiration was measured with glutamate/malate only. Each bar in the graphs represents the mean ± S.E. of 12 *Mclk1*^{+/+} and 10 *Mclk1*^{+/-} animals. The asterisk denotes statistical significance of the difference between *Mclk1*^{+/+} and *Mclk1*^{+/-} animals, $p < 0.05$. H, schematic representation of the electron transport chain in affected tissues of *Mclk1*^{+/-} mice. The rates of oxygen consumption by isolated mitochondria are decreased with complex I-, complex II-, and cytochrome *c*/complex IV-specific substrates (red arrows). The rates of electron transport between complexes I and III as well as between complexes II and III are reduced, as shown in orange arrows. Complex II activity is down-regulated (red arrow), whereas the activities of the other complexes are unaffected (green bars). See Table 1 for complete numerical results.

Defective Mitochondria in Long-lived Mice

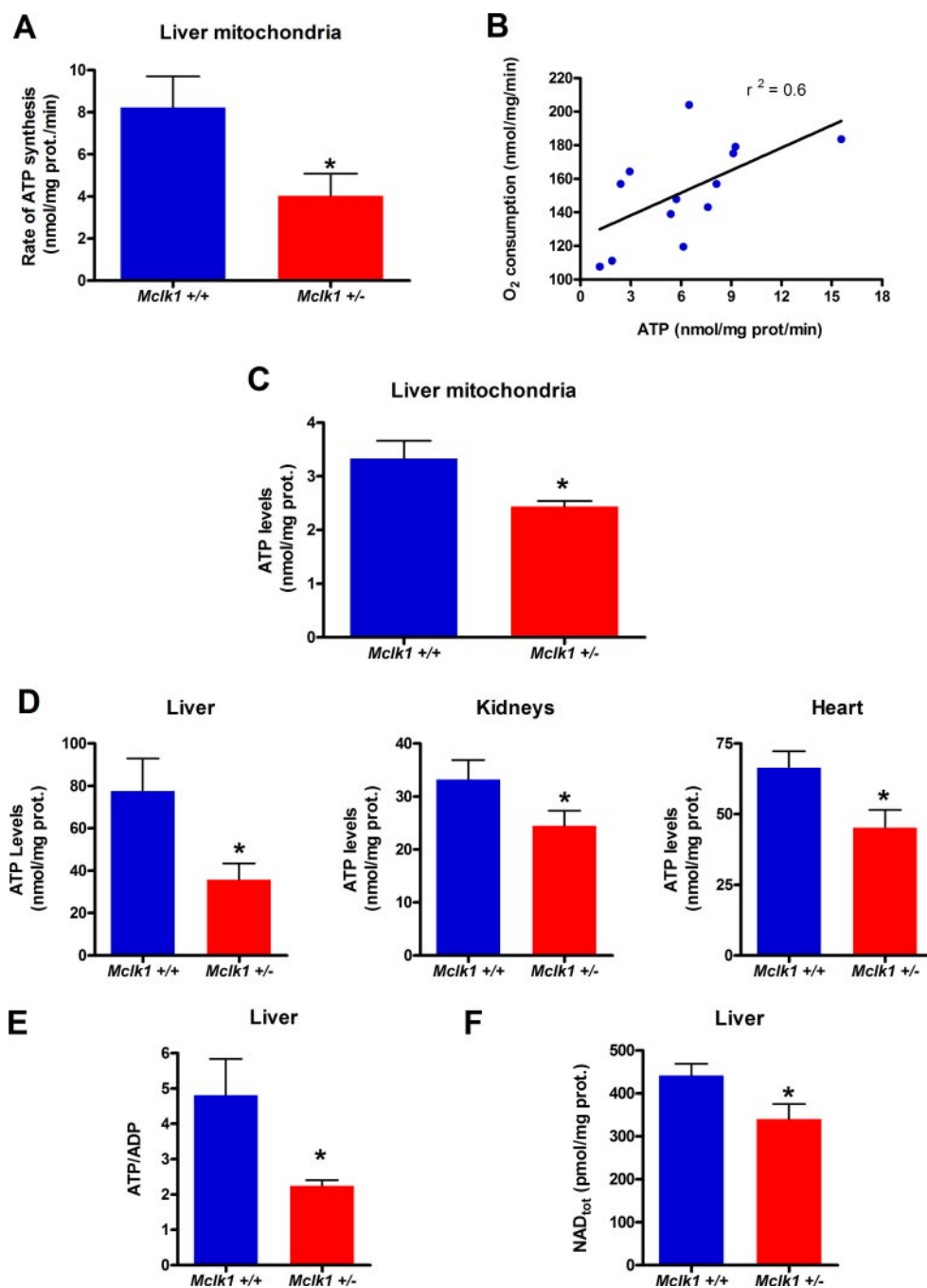


FIGURE 3. Mitochondrial ATP synthesis and cellular ATP and NAD levels are decreased in *Mcl1*^{+/-} mutants. *A*, rates of ATP production by isolated mitochondria from liver of young (3 months) Balb/c males of both genotypes. *B*, correlation between the rates of ATP production and oxygen consumption by mitochondria isolated from individual animals. *C*, ATP levels in freshly isolated liver mitochondria from *Mcl1*^{+/+} and *Mcl1*^{+/-} animals. *D*, cellular ATP levels measured in liver (*, $p < 0.03$), kidney and heart (*, $p < 0.03$) samples of both genotypes. *E*, ATP/ADP ratio measured in liver. *F*, total cellular NAD (NAD⁺, NADH) levels measured in liver. Each bar in the graphs represents the mean \pm S.E. of 6 *Mcl1*^{+/+} and 7 *Mcl1*^{+/-} animals. The asterisk denotes statistical significance of the difference between *Mcl1*^{+/+} and *Mcl1*^{+/-} animals unless stated otherwise $p < 0.05$.

in heterozygous mice (Fig. 3F). Thus, the altered mitochondrial function of *Mcl1*^{+/-} likely affects the rate of a variety of energy-dependent cellular processes by reducing *in vivo* ATP levels as well as total NAD levels.

Altered Activities of the TCA Cycle Enzymes Aconitase and α -Ketoglutarate Dehydrogenase—Next, we tested the activities of the main enzymes of the TCA cycle in the *Mcl1*^{+/-} mutants

(Table 1 and Fig. 4F) and found that the activity of aconitase was severely reduced, whereas that of α -ketoglutarate dehydrogenase, a rate-limiting enzyme regulating the metabolic flux through the cycle, was increased. The other enzymes that were analyzed were unaffected. It is well known that aconitase is particularly susceptible to reaction with superoxide (29), and we believe that the reduction of aconitase is in fact because of an increase of oxidative stress in the mitochondria (see below). Interestingly, it has been predicted that in a situation in which aconitase is depleted due to oxidative stress the TCA cycle might function differently and use α -ketoglutarate dehydrogenase as a pivotal enzyme to produce NADH by way of the α -ketoglutarate produced from glutamate through transamination (30). Thus, the increased level of α -ketoglutarate dehydrogenase that we observe might represent a compensation for the loss of aconitase.

High Oxidative Stress in the Mitochondria of Young Mutants—The loss of aconitase activity, which is a commonly used biomarker of mitochondrial oxidative stress, suggested that *Mcl1*^{+/-} mutants sustain high intramitochondrial oxidative stress. To investigate this possibility, we determined the level of oxidative damage to mitochondrial proteins and mitochondrial lipids. We found that the level of protein carbonylation was increased (Fig. 4A), although the level of lipid peroxidation remained unaffected (Fig. 4B). This apparent discrepancy between protein and lipid oxidative damage could be explained by the different sensitivities of these reactions to the exact ROS species present but also by the fact that proteins appear to be one of the primary targets of mitochondrial ROS (31, 32).

Furthermore, it is well known that cells react to increased oxidative stress by increasing the activity of detoxifying enzymes (33, 34). Thus, we tested two of the principal components of this detoxification system in mitochondria, the glutathione peroxidases and the manganese-dependent superoxide dismutase. All activities were increased in *Mcl1*^{+/-} mutants (Fig. 4, C and D). We also measured the extramitochondrial production of ROS

by isolated mitochondria. Production of ROS by mitochondria is believed to be mostly due to electron transport through the electron transport chain (33, 35). Furthermore, ROS production increases sharply when the rate of electron transport is blocked, for example by treatment with inhibitors (36). We found no difference in the absolute level of ROS produced from *Mclkl*^{+/-} mitochondria (data not shown). However, the level of ROS produced relative to oxygen consumption was increased (Fig. 4E). This suggests that electron transport is less efficient in *Mclkl*^{+/-} mutants in terms of channeling electrons through the electron transport chain while preventing the loss of electrons to superoxide production. Thus, in *Mclkl*^{+/-} mutants, aconitase and mitochondrial proteins in general sustain increased oxidative damage despite the up-regulation of detoxifying enzyme activities, and absolute levels of ROS production by mitochondria are at least as high as in the wild type. Taken together, these results suggest that there is a substantial increase in mitochondrial levels of ROS (Fig. 5H).

Normal or Low Cytoplasmic Oxidative Stress in Young Mutants—Cytoplasmic ROS damage parameters were also measured, but no indication of an increase in cytoplasmic ROS or ROS damage was found (Fig. 5, A–G). In fact, we observed a decrease in protein carbonylation (Fig. 5A). Cytoplasmic lipid peroxidation appeared reduced, but the effect did not reach significance (Fig. 5B). Aconitase activity was also normal (Fig. 5C). It is notable that, because CLK-1/MCLK1 is a mitochondrial protein, the reduced cytoplasmic protein carbonylation is likely a secondary effect of the increased oxidative stress or the decreased electron transport observed in the mitochondria. However, our analysis of detoxifying enzymes (Fig. 5, D and E), which revealed no change in cytoplasmic enzyme activities, suggests that increased protection from cytoplasmic ROS in reaction to the mitochondrial stress is not the mechanism that keeps cytoplasmic carbonylation low. A more likely mechanism is a reduction in the rate of cytoplasmic ROS-producing processes due to the decreased levels of ATP and total NAD in these animals (Figs. 2 and 6).

Reduced Levels of Systemic Oxidative Stress Biomarkers—We carried out two tests for markers of systemic oxidative stress. We measured plasma levels of isoprostanes, which can be secreted into the plasma from multiple tissues as a result of damage to membrane lipids (37). These levels, which are known to increase sharply with age, were reduced in *Mclkl* heterozygotes compared with *Mclkl*^{+/+} (Fig. 5F). As the majority of the oxidative metabolites of lipids that find their way into the plasma do not originate in the mitochondria but in cellular membranes, the reduction observed in young *Mclkl*^{+/-} mutants are likely because of a decrease in cytoplasmic ROS-generating processes (Fig. 6). We also analyzed oxidative damage to DNA by measuring plasma levels of 8-hydroxy-2'-deoxyguanosine, a modified nucleoside base that is present in the plasma, excreted in the urine, and associated with aging (38). Although the levels of 8-hydroxy-2'-deoxyguanosine appear slightly reduced in *Mclkl*^{+/-} animals, we found no significant difference between genotypes (Fig. 5G).

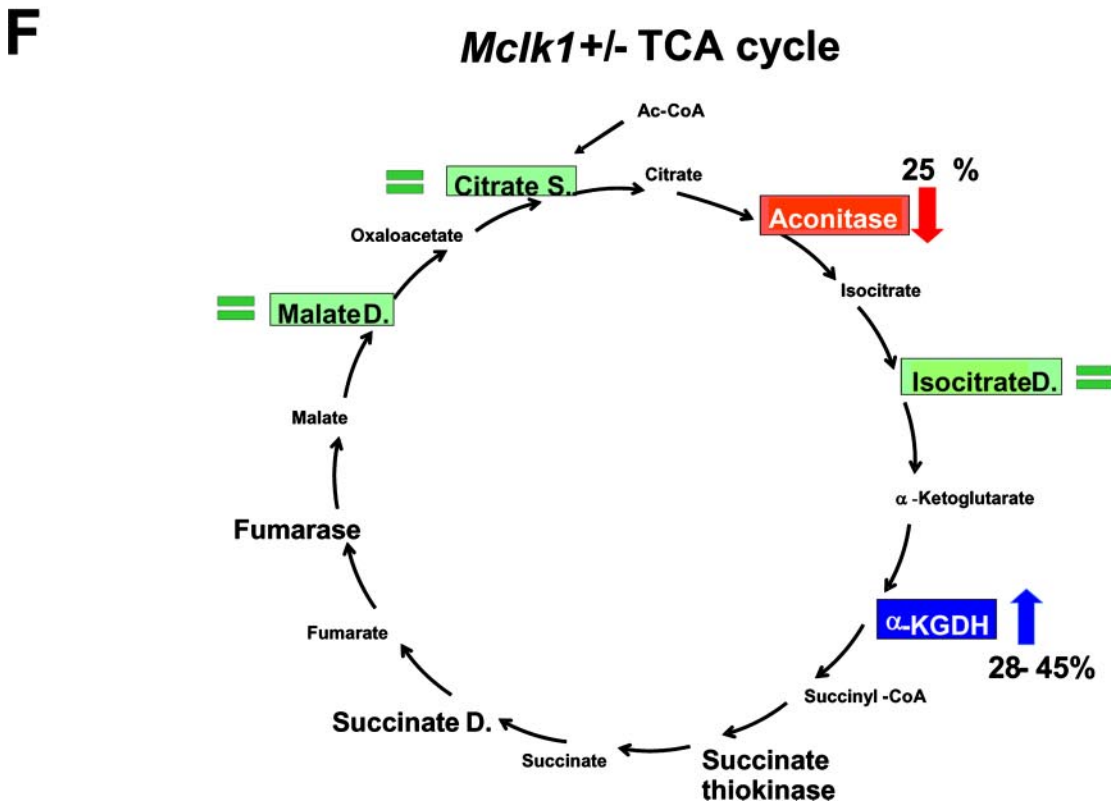
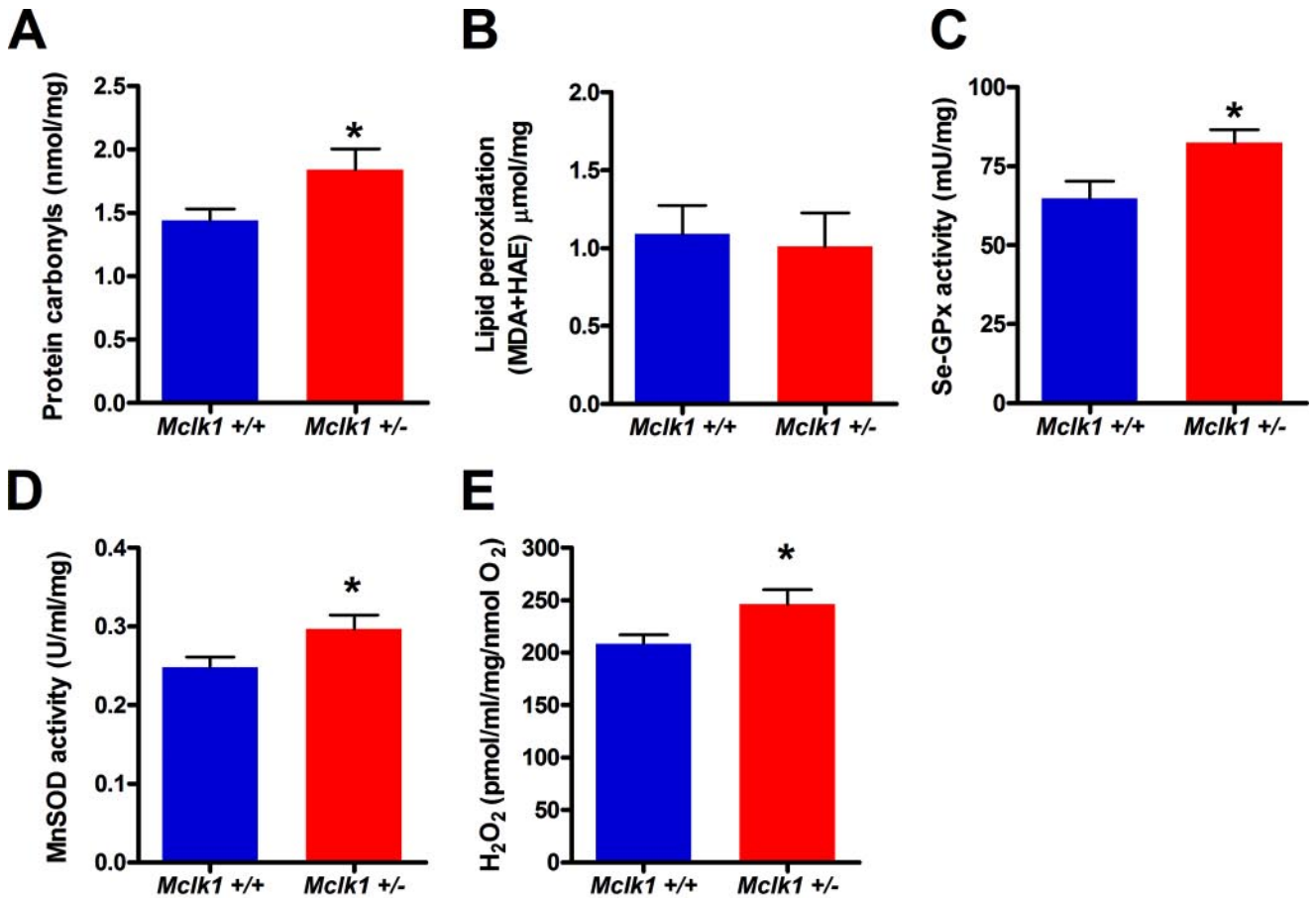
DISCUSSION

Our study strongly suggests that CLK-1/MCLK1 determines lifespan in a ubiquinone-independent manner. Previously, we had

found that UQ levels were reduced in the livers of very old, moribund, *Mclkl*^{+/-} mutants but not in young animals due to the presence in the former of cells that had lost both copies of *Mclkl* by loss-of-heterozygosity (2). At the time, the only documented phenotype of *Mclkl*^{+/-} mutants was their increased lifespan, which could have been the result of the loss of *Mclkl* in very old animals (14). The present findings, however, strongly imply that the well known function of CLK1/MCLK1 in UQ biosynthesis is not linked to the increased lifespan phenotype. Indeed, we find that *Mclkl* heterozygosity affects the function of mitochondria in multiple organs in young animals in the absence of any effect on the levels of UQ (Fig. 1). Mitochondrial function appears very sensitive to the additional activity of MCLK1, as profound effects result from an only 2-fold reduction of wild-type MCLK1. This suggests that this haplo-insufficient function of MCLK1 might not be enzymatic in nature but, rather, involves a stoichiometric relation to other mitochondrial proteins. Our conclusion of a second function for CLK-1/MCLK1 is consistent with a recent study which indicates that exogenous CoQ₁₀ is unable to restore wild-type ATP levels in dissociated cells from *Mclkl*^{-/-} embryos cultured *in vitro* (39).

We have found by several measures that the reduction of MCLK1 levels alters the function of the electron transport chain and, thus, leads to early mitochondrial dysfunction. This defect results in a reduction of energy metabolism as revealed by a lower oxygen consumption rate and a substantial decrease in mitochondrial ATP production as well as in cellular ATP levels. Because ATP is the principal carrier of energy in cells, this reduction is likely to interfere with many important ATP-dependent cellular processes. This hypothesis was quickly confirmed by our finding that cellular levels of total NAD (NAD⁺, NADH), whose generation is dependent on the levels of ATP (40), were significantly decreased in *Mclkl*^{+/-} mutants. It is well established that the NAD⁺/NADH pool plays crucial roles in mediating mitochondrial energy metabolism such as by donating electrons to the electron transport chain or by acting as a coenzyme for rate-limiting TCA cycle enzymes (41). Thus, the decrease in NAD and in ATP levels observed in *Mclkl*^{+/-} mice likely results in a vicious cycle that depresses energy metabolism (Fig. 6A). Moreover, NAD as well as ATP are necessary for the generation of nicotinamide adenine dinucleotide phosphates (including NADP⁺ and NADPH), molecules involved in important cellular functions such as energy metabolism, signal transduction, and calcium homeostasis (42). Interestingly, NADPH is also the coenzyme for many enzymes participating in mitochondrial ROS detoxification, including glutathione reductases, thioredoxin reductases, and cytochrome P450 reductases (43). In fact, it was shown that a diminished NADPH concentration in mitochondria results in an elevated level of ROS damage and a significant reduction of the cellular ATP concentration (44). Therefore, the increase in mitochondrial oxidative stress that occurs in *Mclkl*^{+/-} mice despite the up-regulation of the main antioxidants, especially glutathione peroxidases, could be attributable to a reduction in the formation of NADPH, and this phenomenon could further contribute to the vicious cycle leading to mitochondrial dysfunction (Fig. 6A).

The analysis of the mitochondrial phenotypes of *Mclkl*^{+/-} mutants supports the notion that mitochondrial energy metabo-



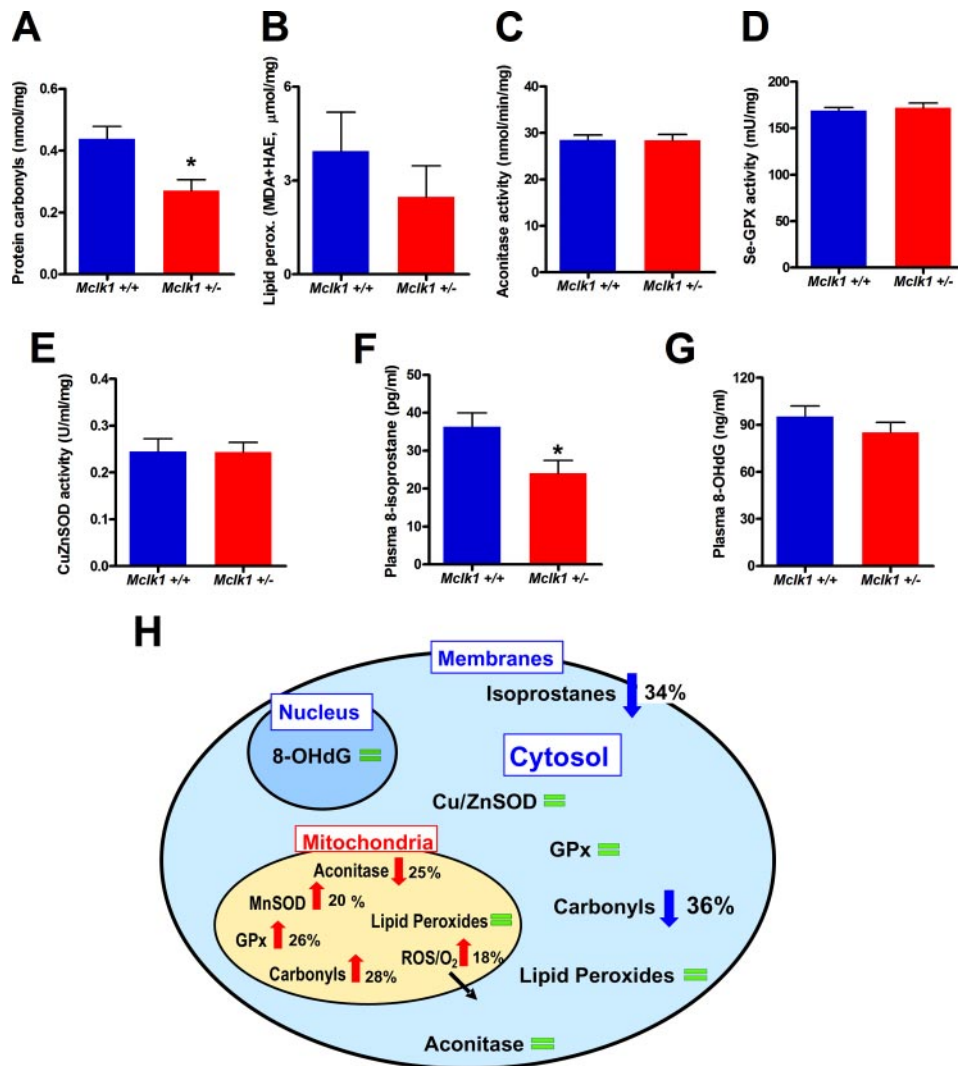


FIGURE 5. Normal or low cytoplasmic and systemic oxidative stress in young *Mclk1*^{+/-} mutants. Analysis of cytoplasmic oxidative stress markers, including the levels of cytoplasmic protein carbonyls (A) (*, $p < 0.01$), lipid peroxidation (B), and aconitase activity (C) as well as glutathione peroxidase (GPx) and copper-zinc superoxide dismutase (Cu,ZnSOD) activities (D–E) revealed low or normal oxidative stress in non-mitochondrial compartments in *Mclk1*^{+/-} mice. MDA, malondialdehyde; HAE, 4-hydroxy-alkenal. Furthermore, the measurement of the levels of plasmatic 8-hydroxy-2'-deoxyguanosine (8-OHdG) (F) and free and etherified isoprostanes (*, $p < 0.03$) (G) also indicate low or normal systemic oxidative stress in *Mclk1*^{+/-} mutants. Each bar in the graphs represents the mean \pm S.E. of 12 *Mclk1*^{+/+} and 10 *Mclk1*^{+/-} animals. The asterisk denotes statistical significance of the difference between *Mclk1*^{+/+} and *Mclk1*^{+/-} animals. H, schematic representation of the effects of *Mclk1* heterozygosity on mitochondrial, cytosolic, and systemic oxidative stress. Changes that indicate the presence of increased oxidative stress are indicated with red arrows, whereas blue arrows indicate changes that indicate low oxidative stress and green bars indicate no difference between genotypes.

lism is crucial to aging. The electron transport chain in mitochondria is the site of ATP production and the main source of energy production in the cells of animals. Therefore, one expects mitochondrial function to be tightly linked to global energy production and utilization. We have found that mitochondrial function as well as ATP and total NAD levels are significantly reduced in young *Mclk1*^{+/-} mutants and further discovered that this decrease is

FIGURE 4. Young *Mclk1*^{+/-} mice have higher mitochondrial oxidative stress and altered TCA cycle. Mitochondria of young *Mclk1*^{+/-} mice display high oxidative stress as revealed by accumulation of protein carbonyls (A), higher levels, but not significantly, of lipid peroxidation (B), up-regulation of the major enzymatic antioxidant defenses, such as Se-GPx (C) and manganese-dependent superoxide dismutase (MnSOD; D), and increased ROS production per molecule of reduced O₂ from isolated mitochondria (E). Each bar in the graphs represents the mean \pm S.E. of 12 *Mclk1*^{+/+} and 10 *Mclk1*^{+/-} animals. The asterisk denotes statistical significance of the difference between *Mclk1*^{+/+} and *Mclk1*^{+/-} animals, $p < 0.05$. F, schematic representation of the effects of *Mclk1* heterozygosity on key TCA cycle enzymes. Aconitase (in red) is partially inactivated, and α -ketoglutarate dehydrogenase (α -KGDH, in blue) is up-regulated in *Mclk1*^{+/-} animals. Unaffected enzymes are shown in green.

linked to lower levels of cytoplasmic oxidative damage and to a reduction in an age-associated systemic biomarkers of oxidative stress to membranes. As *Mclk1*^{+/-} mutants are known to be long-lived, our data supports one aspect of the rate-of-living theory of aging that postulates the existence of a link between energy metabolism and aging (45, 46). Indeed, this theory proposes that what determines the lifespan of an organism is the rate at which it produces and uses energy at the cellular level. This theory was originally mostly supported by the observation that individuals belonging to species that have lower mass-specific metabolic rates tend to live longer than individual belonging to species with higher mass-specific metabolic rates. However, the inferences drawn from data about basal metabolic rates and its scaling in species of different body masses and life spans are now considered flawed by many (45, 46). On the other hand, our current as well as other findings (3, 47, 48) lead to the same conclusion, that is, the importance of energy metabolism, by way of a very different type of evidence.

Interestingly, our observations also suggest that the reduction of *Mclk1* partially mimics some of the downstream effects of caloric restriction, which include reduced metabolism (49) and reduced systemic oxidative damage (50). We also found that TCA cycle enzymes from liver mitochondria of *Mclk1*^{+/-} mutants and mitochondrial antioxidants are regulated in part like those of calorie-restricted rodents (51, 52). Furthermore, given the evolutionary conservation of the action of *clk-1/Mclk1* on lifespan, it is likely relevant that our previous work with *C. elegans* has shown that the effects of caloric restriction and *clk-1* on lifespan are partially redundant (4). However, in contrast to what is observed in calorie-restricted animals (53), we observe an increase in mitochondrial oxidative stress in *Mclk1*^{+/-} mutants. This might indicate that caloric restriction and *Mclk1* converge on the same downstream mecha-

Defective Mitochondria in Long-lived Mice

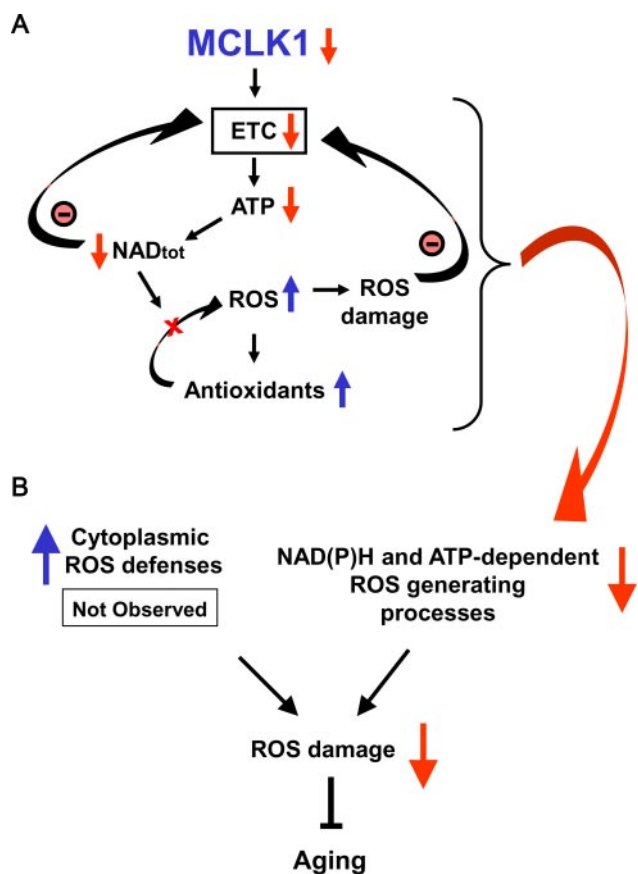


FIGURE 6. Links between the early mitochondrial dysfunction, the attenuation of systemic oxidative stress, and the long-lived phenotype of *Mclk1*^{+/-} mice. *A*, reduction of MCLK1 levels in *Mclk1*^{+/-} mutants reduces electron transport chain function. This results in a reduction in ATP levels, which is likely to have a negative effect on various ATP-dependent mitochondrial and cellular processes such as total nicotinamide adenine dinucleotide, NAD_{tot}, biosynthesis. Because the integrity of the NAD_{tot} (NAD⁺, NADH) pool is crucial for electron transport chain (ETC) function, the resulting reduction in NAD_{tot} levels will also negatively affect mitochondrial energy production, thus creating a vicious cycle. Additionally, the decrease in NAD_{tot} levels will compromise the ROS-detoxifying capacity of crucial mitochondrial NADPH-dependent antioxidants such as the glutathione peroxidases (GPx) that required reduced glutathione generated by glutathione reductase in an NADPH-dependent reaction. This situation leads to an increase in intramitochondrial ROS damage despite an up-regulation of antioxidant activities which can further contribute to reduction in electron transport chain function. *B*, the early mitochondrial dysfunction observed in *Mclk1*^{+/-} mutant is paradoxically linked to a decrease in the levels of cytosolic and systemic oxidative stress. This could be the result of an up-regulation of cytoplasmic antioxidant defenses in response to mitochondrial oxidative stress, but this was not observed. Thus, a more likely mechanism is a reduction in the rate of cytoplasmic ROS-producing oxidases due to the decreased levels of ATP and NAD_{tot}. Because it is well known that systemic oxidative stress is tightly linked to aging, our model could explain how a reduction in MCLK1 levels ultimately slows down the aging process.

nisms but that the reduction in mitochondrial ROS levels observed in calorie-restricted animals might not be the mechanism by which caloric restriction extends life span.

Our results also suggest that mitochondrial oxidative stress is not the link between energy generation and aging. Indeed, a plausible mechanism for the link between energy metabolism and lifespan is the generation of ROS as byproducts of mitochondrial function (46, 54). Mitochondrial ROS can damage mitochondria, and there is a well documented gradual loss of mitochondrial function with chronological age (55, 56). This loss, by impairing adequate cellular energy production, could

be the cause of the dysfunction of senescent cells and organisms. Based on these findings, the mitochondrial oxidative stress theory of aging states that production of ROS during cellular respiration is responsible for the damage associated with the aging process and is a key factor affecting species longevity (57). Experimental evidence in *C. elegans* supports part of this model as it indicates that reduction in mitochondrial electron transport can dramatically prolong worm life span (47, 58). However, this effect in worms is likely not mediated by ROS (48, 58–60). Our findings with *Mclk1* also appear incompatible with the mitochondrial oxidative stress theory of aging. Indeed, we have found that young *Mclk1*^{+/-} mutant mitochondria sustain high oxidative stress, yet their altered function ultimately results in slow aging. The significance of our findings is that, as the *Mclk1*^{+/-} mutants live long and differ minimally from their *Mclk1*^{+/+} siblings at the molecular level (reduced dosage of one naturally encoded gene), it is difficult to conceive of a mechanism by which the same minimal change could both decrease the rate of aging and increase mitochondrial oxidative stress if the latter is the cause of aging.

It is important to note that despite the above considerations, our results remain in line with the overwhelming number of studies which have shown that increased oxidative stress is tightly correlated with the aged phenotype (61). Indeed, this correlation is maintained in our experiments as we find that the phenotype of *Mclk1*^{+/-} mutants is characterized by a low level of non-mitochondrial oxidative damage. In fact, most past observations as well as our current observations are consistent with the notion that increased oxidative stress is a consequence of aging that strongly impinges on the aged phenotype.

Our findings should help to redefine the link between mitochondrial ROS production, non-mitochondrial oxidative stress, and lifespan. In fact, our results are consistent with other studies which have found that early deregulation of mitochondrial ROS production can be associated with increased lifespan. Indeed, elevated ROS production has been measured in isolated mitochondria from long-lived *C. elegans daf-2* mutants, and it has been shown that the rates of mitochondrial H₂O₂ production tended to increase with mean survival in different *Drosophila* lines (62, 63). Another recent study indicates that glucose restriction prolongs *C. elegans* lifespan by inducing mitochondrial ROS production (64). In mammals, it was shown that various tissues of the long-lived naked-mole rats exhibit high oxidative damage, that knock-out mice heterozygous for the mitochondrial manganese-dependent superoxide dismutase showed the expected increases in mitochondrial oxidative stress without any effects on lifespan, and that reduced levels of the antioxidant enzyme GPX4 increases mouse lifespan (65–67). One possibility to explain these striking results is that the increased mitochondrial oxidative stress induces compensatory mechanisms that reduce oxidative stress in other cellular compartments such as in the cytosol, nucleus, and membrane systems and ultimately contribute to the long lifespan phenotype. However, it remains unclear what these compensatory mechanisms would be as we could observe no obvious increase in the activity of cytosolic detoxifying enzymes. Alternatively, slow cellular metabolism due to low ATP synthesis and low ATP levels could result in lower activity of cytoplasmic energy-de-

pendent processes that produce ROS and lead to oxidative stress (Fig. 6B). In addition, low levels of total NAD should negatively affect the activity of extra-mitochondrial NADH/NADPH oxidases, which are known to be major generators of ROS (68, 69) and, thus, also contribute to reduce the accumulation of systemic oxidative damage that is likely involved in the increased lifespan phenotype of the *Mclk1*^{+/-} mice (Fig. 6B).

Acknowledgments—We thank Ève Bigras and Aurélie Masurel for help with animal colony maintenance and genotyping. We thank Zaruhi Stepanyan for preliminary results on aconitase activity. We thank Robyn Branicky for reading the manuscript.

REFERENCES

- Wong, A., Boutis, P., and Hekimi, S. (1995) *Genetics* **139**, 1247–1259
- Liu, X., Jiang, N., Hughes, B., Bigras, E., Shoubridge, E., and Hekimi, S. (2005) *Genes Dev.* **19**, 2424–2434
- Lakowski, B., and Hekimi, S. (1996) *Science* **272**, 1010–1013
- Lakowski, B., and Hekimi, S. (1998) *Proc. Natl. Acad. Sci. U. S. A.* **95**, 13091–13096
- Kenyon, C. (2005) *Cell* **120**, 449–460
- Hekimi, S. (2006) *Nat. Genet.* **38**, 985–991
- Taguchi, A., Wartschow, L. M., and White, M. F. (2007) *Science* **317**, 369–372
- Levavasseur, F., Miyadera, H., Sirois, J., Tremblay, M. L., Kita, K., Shoubridge, E., and Hekimi, S. (2001) *J. Biol. Chem.* **276**, 46160–46164
- Nakai, D., Yuasa, S., Takahashi, M., Shimizu, T., Asaumi, S., Isono, K., Takao, T., Suzuki, Y., Kuroyanagi, H., Hirokawa, K., Koseki, H., and Shirasawa, T. (2001) *Biochem. Biophys. Res. Commun.* **289**, 463–471
- Kayser, E. B., Sedensky, M. M., Morgan, P. G., and Hoppel, C. L. (2004) *J. Biol. Chem.* **279**, 54479–54486
- Hihi, A. K., Kebir, H., and Hekimi, S. (2003) *J. Biol. Chem.* **278**, 41013–41018
- Jonassen, T., Larsen, P. L., and Clarke, C. F. (2001) *Proc. Natl. Acad. Sci. U. S. A.* **98**, 421–426
- Branicky, R., Nguyen, P. A., and Hekimi, S. (2006) *Mol. Cell. Biol.* **26**, 3976–3985
- Aguilaniu, H., Durieux, J., and Dillin, A. (2005) *Genes Dev.* **19**, 2399–2406
- Kwong, L. K., and Sohal, R. S. (1998) *Arch. Biochem. Biophys.* **350**, 118–126
- Starkov, A. A., Fiskum, G., Chinopoulos, C., Lorenzo, B. J., Browne, S. E., Patel, M. S., and Beal, M. F. (2004) *J. Neurosci.* **24**, 7779–7788
- Ellard, J. P., McCudden, C. R., Tanega, C., James, K. A., Ratkovic, S., Staples, J. F., and Wagner, G. F. (2007) *Mol. Cell. Endocrinol.* **264**, 90–101
- Zini, R., Berdeaux, A., and Morin, D. (2007) *Free Radic. Res.* **41**, 1159–1166
- Schuh, R. A., Kristian, T., Gupta, R. K., Flaws, J. A., and Fiskum, G. (2005) *Toxicol. Sci.* **88**, 495–504
- Drew, B., and Leeuwenburgh, C. (2003) *Am. J. Physiol. Regul. Integr. Comp. Physiol.* **285**, 1259–1267
- Sone, H., Sasaki, Y., Komai, M., Toyomizu, M., Kagawa, Y., and Furukawa, Y. (2004) *Biochem. Biophys. Res. Commun.* **314**, 824–829
- Kwong, L. K., and Sohal, R. S. (2000) *Arch. Biochem. Biophys.* **373**, 16–22
- Yu, L., and Yu, C. A. (1982) *J. Biol. Chem.* **257**, 2016–2021
- Nulton-Persson, A. C., and Szweda, L. I. (2001) *J. Biol. Chem.* **276**, 23357–23361
- Muller, F. L., Liu, Y., and Van Remmen, H. (2004) *J. Biol. Chem.* **279**, 49064–49073
- Flohe, L., and Gunzler, W. A. (1984) *Methods Enzymol.* **105**, 114–121
- Crinson, M., and Nicholls, P. (1992) *Biochem. Cell Biol.* **70**, 301–308
- Austin, J., and Aprille, J. R. (1984) *J. Biol. Chem.* **259**, 154–160
- Gardner, P. R., Raineri, I., Epstein, L. B., and White, C. W. (1995) *J. Biol. Chem.* **270**, 13399–13405
- Tretter, L., and Adam-Vizi, V. (2005) *Philos. Trans. R. Soc. Lond. B. Biol. Sci.* **360**, 2335–2345
- Kowaltowski, A. J., and Vercesi, A. E. (1999) *Free Radic. Biol. Med.* **26**, 463–471
- Temple, M. D., Perrone, G. G., and Dawes, I. W. (2005) *Trends Cell Biol.* **15**, 319–326
- Cadenas, E., Boveris, A., Ragan, C. I., and Stoppani, A. O. (1977) *Arch. Biochem. Biophys.* **180**, 248–257
- Franco, A. A., Odom, R. S., and Rando, T. A. (1999) *Free Radic. Biol. Med.* **27**, 1122–1132
- Turrens, J. F., Alexandre, A., and Lehninger, A. L. (1985) *Arch. Biochem. Biophys.* **237**, 408–414
- Turrens, J. F., and Boveris, A. (1980) *Biochem. J.* **191**, 421–427
- Morrow, J. D. (2000) *Drug Metab. Rev.* **32**, 377–385
- Chiou, C. C., Chang, P. Y., Chan, E. C., Wu, T. L., Tsao, K. C., and Wu, J. T. (2003) *Clin. Chim. Acta* **334**, 87–94
- Takahashi, M., Shimizu, T., Moriizumi, E., and Shirasawa, T. (2008) *Mech. Ageing Dev.* **129**, 291–298
- Magni, G., Amici, A., Emanuelli, M., Raffaelli, N., and Ruggieri, S. (1999) *Adv. Enzymol. Relat. Areas Mol. Biol.* **73**, 135–182
- Berger, F., Ramirez-Hernandez, M. H., and Ziegler, M. (2004) *Trends Biochem. Sci.* **29**, 111–118
- Lerner, F., Niere, M., Ludwig, A., and Ziegler, M. (2001) *Biochem. Biophys. Res. Commun.* **288**, 69–74
- Ying, W. (2008) *Antioxid. Redox Signal.* **10**, 179–206
- Jo, S. H., Son, M. K., Koh, H. J., Lee, S. M., Song, I. H., Kim, Y. O., Lee, Y. S., Jeong, K. S., Kim, W. B., Park, J. W., Song, B. J., and Huh, T. L. (2001) *J. Biol. Chem.* **276**, 16168–16176
- Pearl, R. (1922) *The Biology of Death*, J. B. Lippincott, Philadelphia
- Speakman, J. R. (2005) *J. Exp. Biol.* **208**, 1717–1730
- Feng, J., Bussiere, F., and Hekimi, S. (2001) *Dev. Cell* **1**, 633–644
- Yang, W., Li, J., and Hekimi, S. (2007) *Genetics* **177**, 2063–2074
- McCarter, R. J., and McGee, J. R. (1989) *Am. J. Physiol.* **257**, E175–E179
- Lopez-Torres, M., Gredilla, R., Sanz, A., and Barja, G. (2002) *Free Radic. Biol. Med.* **32**, 882–889
- Hagopian, K., Ramsey, J. J., and Weindruch, R. (2004) *Exp. Gerontol.* **39**, 1145–1154
- Sreekumar, R., Unnikrishnan, J., Fu, A., Nygren, J., Short, K. R., Schimke, J., Barazzoni, R., and Nair, K. S. (2002) *Am. J. Physiol.* **283**, E38–E43
- Sohal, R. S., Ku, H. H., Agarwal, S., Forster, M. J., and Lal, H. (1994) *Mech. Ageing Dev.* **74**, 121–133
- Finkel, T., and Holbrook, N. J. (2000) *Nature* **408**, 239–247
- Cadenas, E., and Davies, K. J. (2000) *Free Radic. Biol. Med.* **29**, 222–230
- Shigenaga, M. K., Hagen, T. M., and Ames, B. N. (1994) *Proc. Natl. Acad. Sci. U. S. A.* **91**, 10771–10778
- Harman, D. (1972) *J. Am. Geriatr. Soc.* **20**, 145–147
- Hekimi, S., and Guarente, L. (2003) *Science* **299**, 1351–1354
- Dillin, A., Hsu, A. L., Arantes-Oliveira, N., Lehrer-Graiwer, J., Hsin, H., Fraser, A. G., Kamath, R. S., Ahringer, J., and Kenyon, C. (2002) *Science* **298**, 2398–2401
- Lee, S. S., Lee, R. Y., Fraser, A. G., Kamath, R. S., Ahringer, J., and Ruvkun, G. (2003) *Nat. Genet.* **33**, 40–48
- Sohal, R. S. (2002) *Free Radic. Biol. Med.* **33**, 573–574
- Ballard, J. W., Katewa, S. D., Melvin, R. G., and Chan, G. (2007) *Ann. N. Y. Acad. Sci.* **1114**, 93–106
- Brys, K., Vanfleteren, J. R., and Braeckman, B. P. (2007) *Exp. Gerontol.* **42**, 845–851
- Schulz, T. J., Zarse, K., Voigt, A., Urban, N., Birringer, M., and Ristow, M. (2007) *Cell Metab.* **6**, 280–293
- Andziak, B., O'Connor, T. P., Qi, W., DeWaal, E. M., Pierce, A., Chaudhuri, A. R., Van Remmen, H., and Buffenstein, R. (2006) *Ageing Cell* **5**, 463–471
- Ran, Q., Liang, H., Ikeno, Y., Qi, W., Prolla, T. A., Roberts, L. J., Jr., Wolf, N., VanRemmen, H., and Richardson, A. (2007) *J. Gerontol.* **62**, 932–942
- Williams, M. D., Van Remmen, H., Conrad, C. C., Huang, T. T., Epstein, C. J., and Richardson, A. (1998) *J. Biol. Chem.* **273**, 28510–28515
- Bedard, K., and Krause, K. H. (2007) *Physiol. Rev.* **87**, 245–313
- Maia, L., Vala, A., and Mira, L. (2005) *Free Radic. Res.* **39**, 979–986